IEEE Access
Multidisciplinary : Rapid Review : Open Access Journal

Received August 7, 2018, accepted September 11, 2018, date of publication October 1, 2018, date of current version October 25, 2018.

Digital Object Identifier 10.1109/ACCESS.2018.2873453

A Fractional Programming Method for Target Localization in Asynchronous Networks

GANG WANG[1], (Member, IEEE), NIRWAN ANSARI[2], (Fellow, IEEE), AND YOUMING LI[1]
[1]Faculty of Electrical Engineering and Computer Science, Ningbo University, Ningbo 315211, China
[2]Advanced Networking Laboratory, Department of Electrical and Computer Engineering, New Jersey Institute of Technology, Newark, NJ 07102, USA

Corresponding author: Gang Wang (wanggang@nbu.edu.cn)

This work was supported in part by the National Natural Science Foundation of China under Grant 61571249, in part by the Zhejiang Provincial Natural Science Foundation under Grant LY18F010011, and in part by the K. C. Wong Magna Fund in Ningbo University.

ABSTRACT In this paper, we address the target device localization problem in the asynchronous networks. For the purpose of saving power resources, the target device is not synchronized with the anchor nodes, but is only required to listen to the signals transmitted from the anchors, which, however, introduces two extra nuisance parameters: the target's clock skew and clock offset. By transforming the time-of-arrival measurements into time-difference-of-arrival measurements, the clock offset of the target's clock is eradicated. However, there still exists the unknown clock skew, which may degrade the localization performance. Since the range of the clock skew is usually known as *a priori*, we assume that it follows a uniform distribution within this range. By doing so, we take it as a part of measurement noise and estimate the target node position only. To estimate the target node position, we formulate a fractional programming problem and further show that it can be solved by solving one single mixed semidefinite and second-order cone program (SD/SOCP). Simulation results illustrate the superior performance of the proposed method over the existing methods.

INDEX TERMS Fractional programming (FP), localization, time-of-arrival (TOA), time-difference-of-arrival (TDOA).

I. INTRODUCTION

Localization has received much attention in recent years owing to its extensive applications in many fields and various networks such as transportation, target tracking, surveillance, and emergency rescue response [1], [2]. Traditionally, the localization problem can be categorized into two classes: time-based and feature-based. The former class utilizes time related information to localize the target. This class requires high-precision time synchronization but provides high localization accuracy; time-of-arrival (TOA) based localization [3]–[6] and time-difference-of-arrival (TDOA) based localization [7]–[10] belong to this class. The latter class utilizes the features of the received signals. This class does not require time synchronization and only requires to compute the power of received signals, i.e., the received signal strength (RSS) [11]–[15]; however, it cannot provide accurate and reliable localization due to strong shadowing effect in urban and indoor areas, although some newly proposed methods using RSS have improved the localization precision [14], [15]. Hence, RSS-based localization cannot meet the requirement of high-precision localization. On the other hand, traditional TOA- and TDOA-based localization require the target device to send or broadcast signals to the anchors, which may quickly drain the power resources of the target.

In this paper, we focus on the high-precision target device localization with relatively low power cost. A typical application is the target device localization in the Internet of Things (IOT) [16], in which the device is usually equipped with simple chips. We utilize a trade-off approach to achieve this aim. In this approach, the anchors are assumed to be time synchronized, which can be easily realized in some available systems, e.g., time synchronization among base stations can be easily implemented in the cellular system. However, different from the traditional TOA- and TDOA-based localization, the target only needs to listen to the anchors and record the arrival time of the signals from the anchors. Apparently, it saves much power since the target does not transmit signals. Moreover, it does not require the target to be time synchronized with the anchors. However, it introduces two extra nuisance

2169-3536 © 2018 IEEE. Translations and content mining are permitted for academic research only.
Personal use is also permitted, but republication/redistribution requires IEEE permission.
See http://www.ieee.org/publications_standards/publications/rights/index.html for more information.

parameters due to the unsynchronized target: the skew and the offset of the clock on the target [17], which will make the localization problem more difficult.

A common approach to deal with the unknown clock skew and clock offset is to jointly estimate these parameters and the target position, which is usually referred to as joint synchronization and localization. Various TOA-based joint synchronization and localization methods have been proposed. Zheng and Wu [18] addressed the TOA-based localization problem, in which they assume that the anchors are synchronized, and the clock skew and the clock offset of the target's clock and the target position are jointly estimated. Ahmad *et al.* [19] proposed two methods to tackle the joint time synchronization and target localization problem using TOA measurements. One is called the Expectation-Maximization (EM) method, and the other is the more computationally efficient least squares (LS) method. Wang *et al.* [20] proposed to localize a target by using the two-way TOA (TW-TOA) measurements, in which the anchors and the target are required to record the time stamps to compute the TW-TOA measurements. More importantly, they proposed a procedure to avoid the internal attacks of the network. Gholami *et al.* [21] proposed a new TW-TOA measurement model, in which only the target is required to record the time stamps and the clock offset is eliminated. However, this model introduces some unknown auxiliary variables, i.e., the turn-around times, which have to be dealt with. They first estimated these unknown variables and then using the estimates, they introduced and solved two suboptimal problems, i.e., the generalized trust region (GTR) subproblem and the linear least squares (LLS) problem, to jointly estimate the clock skew and the target position. Gao *et al.* [22] proposed a different way to address the unknown turn-around times, which are taken as nuisance parameters, and proposed a robust least squares method to estimate the target position only. More recently, Vaghefi and Buehrer [23] proposed a semidefinite relaxation (SDR) method to solve the cooperative joint synchronization and TOA-based localization problem by leveraging synchronous anchors. Cooperation of the sensor nodes significantly improves the synchronization and localization performance.

All the above localization methods are derived based on the TOA measurement models. Different from these works, Gholami *et al.* [24] proposed to transform the TOA measurement model into a TDOA measurement model. During the transformation, the clock offset of the target's clock is removed, and the target position and the clock skew are jointly estimated. In this paper, we employ the same idea of transforming the TOA measurements into TDOA measurements. However, unlike the way of addressing the clock skew in [24], we do not estimate the clock skew but take it as a random variable. Since its range is usually known *a priori*, we assume that it follows a uniform distribution within this range. By doing so, we can take it as a part of measurement noise, and thus we only need to estimate the target position. Moreover, we propose a novel fractional programming (FP) method to estimate the target position. In particular, we formulate the localization problem as a fractional program. It is, however, difficult to solve the FP problem owing to its non-convex nature. Performing semidefinite relaxation to the FP results in a quasi-convex problem, which can be solved efficiently in a globally optimal manner. To further reduce the computational complexity, we prove that the quasi-convex problem is equivalent to a mixed semidefinite and second-order cone program (SD/SOCP), which can be solved more efficiently. More importantly, the relaxed quasi-convex problem is quite tight such that it does not require any postprocessing techniques to be further tightened.

The contributions of this work are twofold:

1. We propose a new method to localize a target device with high localization accuracy and relatively low power cost.

2. We propose a novel FP method to solve the localization problem, and it does not require any further postprocessing.

The rest of this paper is organized as follows. In Section II, the measurement model is introduced. The FP method is presented in Section III. Section IV derives the Cramer-Rao lower bound (CRLB) and presents the Mean Square Error (MSE) analysis. Next, the simulation results are illustrated in Section V, and finally, the conclusion is drawn in Section VI.

The following notations will be adopted throughout the article. Bold face lower case letters and bold face upper case letters denote vectors and matrices, respectively. $A_{i,j}$ denotes the (i, j)th element of matrix $\boldsymbol{A}$ and $\boldsymbol{A}_{1:k,j}$ denotes a vector formed by the elements at rows from 1 to k and column j. $\mathbf{0}_{k\times\ell}$ denotes the $k \times \ell$ all-zero matrix; $\mathbf{1}_k$ and $\boldsymbol{I}_k$ denote the $k \times \ell$ all-one column vector and the $k \times k$ identity matrix, respectively. $\otimes$ denotes the Kronecker product. $\mathbb{E}_{\boldsymbol{n}}[\cdot]$ refers to the expectation with respect to $\boldsymbol{n}$. $\text{diag}\{a_1, \ldots, a_\ell\}$ denotes the $\ell \times \ell$ diagonal matrix with $a_1, \ldots, a_\ell$ on the diagonal. $\text{Tr}(\boldsymbol{A})$ and $\text{rank}(\boldsymbol{A})$ stand for the trace and rank of $\boldsymbol{A}$, respectively. For matrix $\boldsymbol{A}$ and $\boldsymbol{B}$, $\boldsymbol{A} \succeq \boldsymbol{B}$ means that $\boldsymbol{A} - \boldsymbol{B}$ is positive semidefinite.

II. MEASUREMENT MODEL

A. MEASUREMENT MODEL

Consider an ℓ-dimensional ($\ell = 2$ or 3) wireless network with $N + 1$ anchors and one target device. The anchor positions are known, which are denoted by $\boldsymbol{s}_i \in \mathbb{R}^\ell$ for $i = 0, \ldots, N$, and the target position is unknown, which is denoted by $\boldsymbol{x}^o \in \mathbb{R}^\ell$. We assume that the anchors are synchronized with a reference clock, while the target is not synchronized. The local time of the target can be denoted by the following affine model:

$$C(t) = wt + \theta \tag{1}$$

where t is the reference time, and w and θ are the clock skew and the clock offset of the target's clock, respectively.

Assume that the target measures the ranges to the anchors by performing the one-way ranging protocol. The process of measurement is conducted as follows. The anchors send their signals to the target at time T_0^k, $k = 1, 2, \ldots, K$ for K times, and the target detects the signals and records the TOAs.

Based on this measurement process, the TOA measurements can be denoted by:

$$t_i^k = w(T_0^k + \|\boldsymbol{x}^o - \boldsymbol{s}_i\|/c + \tilde{n}_i^k) + \theta,\quad i = 0, \ldots, N, \quad k = 1, \ldots, K \tag{2}$$

where c and $\tilde{n}_i^k$ are the speed of light and the measurement noise, respectively. Here, the measurement noise $\tilde{n}_i^k$ is assumed to follow the Gaussian distribution with mean zero and variance $(\tilde{\sigma}_i^k)^2$, i.e., $\tilde{n}_i^k \sim \mathcal{N}(0, (\tilde{\sigma}_i^k)^2)$.

It is worth noting that if the target sends signals to the anchors, then the problem of clock imperfection of the target will not exist because the anchors are time synchronized. However, this measurement procedure consumes more power of the target during the process of sending signals, thus quickly draining the power resources of the target. Moreover, this measurement procedure requires a fusion center to process the measurement data and to send the target position estimate back to the target [24]. In comparison, the measurement procedure adopted in this paper only requires the target to listen to the broadcasting signals transmitted from the anchors, and hence consumes much less power of the target.

B. COPING WITH THE NUISANCE PARAMETERS

Our aim is to estimate the target position under the assumption that the nuisance parameters T_0^k, w, and θ are unknown. There are generally two ways to cope with these nuisance parameters. One way is to jointly estimate all these parameters and the target position. However, from the CRLB analysis, the mean square errors of T_0^k and θ estimates are not lower bounded, implying that we cannot estimate T_0^k and θ separately. Instead, we can only jointly estimate $\boldsymbol{x}^o$, w, and $wT_0^k + \theta$. However, this joint estimation problem involves solving an optimization problem with $\ell+1+K$ variables; it is thus a more difficult problem that cannot be solved efficiently. Thus, we adopt the other way, i.e., removing these parameters by subtracting a reference measurement [24]. Without loss of generality, we choose the zeroth measurement as the reference measurement ($\boldsymbol{s}_0$ is the reference anchor accordingly) in each measurement period, and form the following transformed TDOA measurements:

$$c(t_i^k - t_0^k) = w\left[\|\boldsymbol{x}^o - \boldsymbol{s}_i\| - \|\boldsymbol{x}^o - \boldsymbol{s}_0\| + c(\tilde{n}_i^k - \tilde{n}_0^k)\right],\quad i = 1, \ldots, N, \quad k = 1, \ldots, K, \tag{3}$$

which can further be written as

$$\begin{aligned} d_i^k &= w\left(\|\boldsymbol{x}^o - \boldsymbol{s}_i\| - \|\boldsymbol{x}^o - \boldsymbol{s}_0\| + n_i^k\right) \\ &= w\left(r_i^o - r_0^o + n_i^k\right), \quad i = 1, \ldots, N,\ k = 1, \ldots, K, \end{aligned} \tag{4}$$

with $r_i^o = \|\boldsymbol{x}^o - \boldsymbol{s}_i\|$, $i = 1, \ldots, N$, $r_0^o = \|\boldsymbol{x}^o - \boldsymbol{s}_0\|$, $d_i^k = c(t_i^k - t_0^k)$ and $n_i^k = c(\tilde{n}_i^k - \tilde{n}_0^k)$. By stacking n_i^k for $i = 1, \ldots, N$ and $k = 1, \ldots, K$ into a vector $\boldsymbol{n} = [n_1^1, \ldots, n_N^1, \ldots, n_1^K, \ldots, n_N^K]^T$, $\boldsymbol{n}$ follows the Gaussian distribution with mean zero and covariance $\boldsymbol{Q}$, where $\boldsymbol{Q} = c^2\text{diag}\left\{(\tilde{\sigma}_1^1)^2, \ldots, (\tilde{\sigma}_N^1)^2 \ldots, (\tilde{\sigma}_1^K)^2, \ldots, (\tilde{\sigma}_N^K)^2\right\}$.

From (4), we see that the clock skew w still remains in the localization process. Based on the transformed measurement model, Gholami *et al.* [24] proposed to jointly estimate the clock skew and the target position. In this paper, we propose a novel method to address the nuisance parameter w, which will be detailed in the next section.

III. FRACTIONAL PROGRAMMING

We make the following assumptions on the clock skew w and the noise n_i^k.

Assumption A: We assume that $w = 1 + \delta$ because the value of w is around 1, and $|\delta|$ is upper-bounded by a known constant δ_{max}, i.e., $|\delta| \leq \delta_{max}$.

Assumption B: The value of n_i^k is much smaller than the range between the target and the reference node, i.e., $|n_i^k| \ll \|\boldsymbol{x}^o - \boldsymbol{s}_0\|$.

Note that these are very common assumptions made in the literature, e.g., [7], [24], and [25]. For Assumption A, the value of δ_{max} can be determined by the technical specifications of the crystal oscillator embedded in the sensor node. For Assumption B, if this assumption is not satisfied, the measurements would be erroneous, and are thus useless.

By using $w = 1 + \delta$, (4) can be approximately written as

$$(1 - \delta)d_i^k \approx \|\boldsymbol{x}^o - \boldsymbol{s}_i\| - \|\boldsymbol{x}^o - \boldsymbol{s}_0\| + n_i^k, \quad i = 1, \ldots, N, \tag{5}$$

where the approximation $1/w \approx 1 - \delta$ is used.

By moving δd_i^k to the right-hand side, (5) can be written as

$$d_i^k \approx \|\boldsymbol{x}^o - \boldsymbol{s}_i\| - \|\boldsymbol{x}^o - \boldsymbol{s}_0\| + n_i^k + \delta d_i^k, \quad i = 1, \ldots, N. \tag{6}$$

Note that the approximate measurement model (6) is similar to that adopted in [25], which is the measurement model under the non-line-of-sight (NLOS) condition. Hence, the two robust methods in [25], which take the NLOS errors as nuisance parameters, can naturally be applied to solve the problem in this work. However, the comparison between the measurement model (6) and the model in [25] reveals their differences. The NLOS errors in the model in [25] can be much larger than the noise, while δd_i^k in (6) is relatively small and is on the magnitude of the noise. Based on this observation, we adopt an approach different from that in [25] to handle the term δd_i^k, i.e., we take δ as a random variable and the term δd_i^k as part of the noise. Since the magnitude of δd_i^k is not as large as the NLOS errors, the localization performance will not be degraded much even with inaccurate statistical information of δ. In contrast, the NLOS errors considered in [25] cannot be tackled in this manner because the NLOS errors can be much greater than the noise.

By letting $e_i^k = n_i^k + \delta d_i^k$, (6) becomes

$$\begin{aligned} d_i^k &\approx \|\boldsymbol{x}^o - \boldsymbol{s}_i\| - \|\boldsymbol{x}^o - \boldsymbol{s}_0\| + n_i^k + \delta d_i^k \\ &= \|\boldsymbol{x}^o - \boldsymbol{s}_i\| - \|\boldsymbol{x}^o - \boldsymbol{s}_0\| + e_i^k, \quad i = 1, \ldots, N. \end{aligned} \tag{7}$$

Obviously, if we take δ as a random variable, then e_i^k can be seen as a new random variable. Moreover, it is reasonable to assume that n_i^k and δ are independent. Assume that δ has zero mean and variance σ_δ^2. By stacking e_i^k and d_i^k for $i = 1, \ldots, N$ and $k = 1, \ldots, K$ into vectors $\boldsymbol{e}$ and $\boldsymbol{d}$, respectively, we have $\boldsymbol{e} = \boldsymbol{n} + \delta\boldsymbol{d}$. Obviously, $\boldsymbol{e}$ has mean zero and covariance $\boldsymbol{R}$, where $\boldsymbol{R} = \boldsymbol{Q} + \sigma_\delta^2 \boldsymbol{d}\boldsymbol{d}^T$.

In the following, we present a novel FP method to solve this problem.

By moving $\|\boldsymbol{x}^o - \boldsymbol{s}_i\|$ to the left-hand side in (7) and squaring both sides, we have

$$(d_i^k)^2 - 2d_i^k\|\boldsymbol{x}^o - \boldsymbol{s}_i\| - 2(\boldsymbol{s}_i - \boldsymbol{s}_0)^T\boldsymbol{x} + \|\boldsymbol{s}_i\|^2 - \|\boldsymbol{s}_0\|^2 \approx -2\|\boldsymbol{x}^o - \boldsymbol{s}_0\|e_i^k + (e_i^k)^2. \quad (8)$$

Since δ is typically small, $|\delta d_i^k| \ll \|\boldsymbol{x}^o - \boldsymbol{s}_0\|$ usually holds. Combining this fact and Assumption A, we have $|e_i^k| \ll \|\boldsymbol{x}^o - \boldsymbol{s}_0\|$. Thus, we can neglect the second-order noise terms $(e_i^k)^2$ for $i = 1, \ldots, N$ and $k = 1, \ldots, K$. Dividing both sides by $-2\|\boldsymbol{x}^o - \boldsymbol{s}_0\|$, we have

$$e_i^k \approx \frac{(d_i^k)^2 - 2d_i^k\|\boldsymbol{x}^o - \boldsymbol{s}_i\| - 2(\boldsymbol{s}_i - \boldsymbol{s}_0)^T\boldsymbol{x}^o + \|\boldsymbol{s}_i\|^2 - \|\boldsymbol{s}_0\|^2}{-2\|\boldsymbol{x}^o - \boldsymbol{s}_0\|} \triangleq \theta_i^k(\boldsymbol{x}^o). \quad (9)$$

Based on (9), we can formulate an approximate weighted least squares (WLS) problem:

$$\min_{\boldsymbol{x}} f(\boldsymbol{x}) \triangleq \boldsymbol{\theta}(\boldsymbol{x})^T\boldsymbol{R}^{-1}\boldsymbol{\theta}(\boldsymbol{x}), \quad (10)$$

where $\boldsymbol{\theta}(\boldsymbol{x}) = [\theta_1^1(\boldsymbol{x}), \ldots, \theta_N^1(\boldsymbol{x}), \ldots, \theta_1^K(\boldsymbol{x}), \ldots, \theta_N^K(\boldsymbol{x})]^T$.

Problem (10) can be equivalently written as

$$\min_{\boldsymbol{y}} \frac{(\boldsymbol{A}\boldsymbol{y} - \boldsymbol{b})^T\boldsymbol{R}^{-1}(\boldsymbol{A}\boldsymbol{y} - \boldsymbol{b})}{4\|\boldsymbol{x} - \boldsymbol{s}_0\|^2} \quad \text{s.t. } \|\boldsymbol{x} - \boldsymbol{s}_i\| = r_i, \quad i = 1, \ldots, N, \quad (11)$$

where $\boldsymbol{y} = [\boldsymbol{x}^T \ \boldsymbol{r}^T]^T$ is the optimization variable vector,

$$\boldsymbol{A} = \begin{bmatrix} -2(\boldsymbol{s}_1 - \boldsymbol{s}_0)^T & -2d_1^1 & 0 & \cdots & 0 \\ -2(\boldsymbol{s}_2 - \boldsymbol{s}_0)^T & 0 & -2d_2^1 & \ddots & 0 \\ \vdots & \vdots & \vdots & \ddots & \vdots \\ -2(\boldsymbol{s}_N - \boldsymbol{s}_0)^T & 0 & 0 & \cdots & -2d_N^1 \\ \vdots & \vdots & \vdots & \vdots & \vdots \\ -2(\boldsymbol{s}_1 - \boldsymbol{s}_0)^T & -2d_1^K & 0 & \cdots & 0 \\ -2(\boldsymbol{s}_2 - \boldsymbol{s}_0)^T & 0 & -2d_2^K & \ddots & 0 \\ \vdots & \vdots & \vdots & \ddots & \vdots \\ -2(\boldsymbol{s}_N - \boldsymbol{s}_0)^T & 0 & 0 & \cdots & -2d_N^K \end{bmatrix},$$

and

$$\boldsymbol{b} = \begin{bmatrix} \|\boldsymbol{s}_0\|^2 - \|\boldsymbol{s}_1\|^2 - (d_1^1)^2 \\ \|\boldsymbol{s}_0\|^2 - \|\boldsymbol{s}_2\|^2 - (d_2^1)^2 \\ \vdots \\ \|\boldsymbol{s}_0\|^2 - \|\boldsymbol{s}_N\|^2 - (d_N^1)^2 \\ \vdots \\ \|\boldsymbol{s}_0\|^2 - \|\boldsymbol{s}_1\|^2 - (d_1^K)^2 \\ \|\boldsymbol{s}_0\|^2 - \|\boldsymbol{s}_2\|^2 - (d_2^K)^2 \\ \vdots \\ \|\boldsymbol{s}_0\|^2 - \|\boldsymbol{s}_N\|^2 - (d_N^K)^2 \end{bmatrix}.$$

To facilitate the following relaxation, we rewrite Problem (11) as

$$\min_{\boldsymbol{y}} \frac{(\boldsymbol{A}\boldsymbol{y} - \boldsymbol{b})^T\boldsymbol{R}^{-1}(\boldsymbol{A}\boldsymbol{y} - \boldsymbol{b})}{4\|\boldsymbol{B}\boldsymbol{y} - \boldsymbol{s}_0\|^2} \quad \text{s.t. } \|\boldsymbol{B}\boldsymbol{y} - \boldsymbol{s}_i\| = y_{\ell+i}, \quad i = 1, \ldots, N, \quad (12)$$

where $\boldsymbol{B} = [\boldsymbol{I}_\ell \ \ \boldsymbol{0}_{\ell\times N}]$.

By introducing $\boldsymbol{Y} = \boldsymbol{y}\boldsymbol{y}^T$ and $\boldsymbol{Z} = [\boldsymbol{Y} \ \boldsymbol{y}; \boldsymbol{y}^T \ 1]$, Problem (12) can be equivalently written as

$$\begin{aligned} \min_{\boldsymbol{Z}} \ & \frac{\mathrm{Tr}(\boldsymbol{F}\boldsymbol{Z})}{\mathrm{Tr}(\boldsymbol{D}_0\boldsymbol{Z})} \\ \text{s.t. } & Z_{i+\ell,i+\ell} = \mathrm{Tr}(\boldsymbol{D}_i\boldsymbol{Z}), \quad i = 1, \ldots, N, & (13a) \\ & Z_{N+\ell+1,N+\ell+1} = 1, & (13b) \\ & \boldsymbol{Z} \succeq 0, & (13c) \\ & \mathrm{rank}(\boldsymbol{Z}) = 1, & (13d) \end{aligned}$$

where

$$\boldsymbol{F} = \begin{bmatrix} \boldsymbol{A}^T\boldsymbol{R}^{-1}\boldsymbol{A} & -\boldsymbol{A}^T\boldsymbol{R}^{-1}\boldsymbol{b} \\ -\boldsymbol{b}^T\boldsymbol{R}^{-1}\boldsymbol{A} & \boldsymbol{b}^T\boldsymbol{R}^{-1}\boldsymbol{b} \end{bmatrix},$$

$$\boldsymbol{D}_0 = 4\begin{bmatrix} \boldsymbol{B}^T\boldsymbol{B} & -\boldsymbol{B}^T\boldsymbol{s}_0 \\ -\boldsymbol{s}_0^T\boldsymbol{B} & \|\boldsymbol{s}_0\|^2 \end{bmatrix},$$

$$\boldsymbol{D}_i = \begin{bmatrix} \boldsymbol{B}^T\boldsymbol{B} & -\boldsymbol{B}^T\boldsymbol{s}_i \\ -\boldsymbol{s}_i^T\boldsymbol{B} & \|\boldsymbol{s}_i\|^2 \end{bmatrix}, \quad i = 1, \ldots, N. \quad (14)$$

Problem (13) is a non-convex problem due to the following: (1) the objective function is non-convex, but is quasi-convex; (2) the rank-1 constraint is non-convex. To make this problem tractable, we propose to yield the following problem by dropping the rank-1 constraint:

$$\boldsymbol{Z}^* = \arg\min_{\boldsymbol{Z}} \frac{\mathrm{Tr}(\boldsymbol{F}\boldsymbol{Z})}{\mathrm{Tr}(\boldsymbol{D}_0\boldsymbol{Z})} \quad \text{s.t. } (13a) - (13c), \quad (15)$$

where $\boldsymbol{Z}^*$ denotes the optimal solution of Problem (15).

According to [25], the relaxed problem (15) is not quite tight such that the rank of $\boldsymbol{Z}^*$ is much higher than 1. To alleviate this problem, we utilize the same procedure as that in [25] to tighten Problem (15). Particularly, we add some second-order cone constraints $\|\boldsymbol{x}-\boldsymbol{s}_i\| \leq r_i$ (i.e., $\|\boldsymbol{Z}_{1:\ell,N+\ell+1}-\boldsymbol{s}_i\| \leq Z_{i+\ell,N+\ell+1}$) for $i = 1, \ldots, N$ to Problem (15), thus yielding the following much tighter problem:

$$
\begin{aligned}
\boldsymbol{Z}^* = \arg\min_{\boldsymbol{Z}} \ & \frac{\mathrm{Tr}(\boldsymbol{F}\boldsymbol{Z})}{\mathrm{Tr}(\boldsymbol{D}_0\boldsymbol{Z})} \\
\text{s.t. } & (13a) - (13c), \\
& \|\boldsymbol{Z}_{1:\ell,N+\ell+1} - \boldsymbol{s}_i\| \leq Z_{i+\ell,N+\ell+1}, \\
& i = 1, \ldots, N. \qquad (16)
\end{aligned}
$$

Note that Problem (16) is a quasi-convex problem since the objective function is quasi-convex and the constraint set is convex [26], and it can be solved in a globally optimal manner by the bisection method in which a sequence of SDP feasibility problems need to be solved [26]. However, we show that the problem is equivalent to a mixed SD/SOCP, which means that the globally optimal solution of (16) can be obtained by solving one mixed SD/SOCP.

Proposition 1: The quasi-convex problem (16) can be equivalently transformed to the following mixed SD/SOCP

$$
\begin{aligned}
\min_{\boldsymbol{U}} \ & Tr(\boldsymbol{F}\boldsymbol{U}) \\
s.t. \ & Tr(\boldsymbol{D}_0\boldsymbol{U}) = 1, & (17a) \\
& U_{i+\ell,i+\ell} = Tr(\boldsymbol{D}_i\boldsymbol{U}), \quad i = 1, \ldots, N, & (17b) \\
& U_{N+\ell+1,N+\ell+1} > 0, & (17c) \\
& \boldsymbol{U} \succeq 0, & (17d) \\
& \|\boldsymbol{U}_{1:\ell,N+\ell+1} - \boldsymbol{s}_i U_{N+\ell+1,N+\ell+1}\| \leq U_{i+\ell,N+\ell+1}, \\
& i = 1, \ldots, N. & (17e)
\end{aligned}
$$

Moreover, by denoting $\boldsymbol{U}^*$ as the optimal solution of (17), the optimal solution of (15) can be obtained through the following relation:

$$\boldsymbol{Z}^* = \boldsymbol{U}^*/U^*_{N+\ell+1,N+\ell+1}. \qquad (18)$$

Proof: On one hand, for any feasible solution $\boldsymbol{U}$ of Problem (17), we can always define a point $\bar{\boldsymbol{Z}} = \boldsymbol{U}/U_{N+\ell+1,N+\ell+1}$ since $U_{N+\ell+1,N+\ell+1} > 0$. It is easy to show that $\bar{\boldsymbol{Z}}$ is feasible for Problem (16) and has the same objective value $\mathrm{Tr}(\boldsymbol{F}\boldsymbol{U}) = \mathrm{Tr}(\boldsymbol{F}\bar{\boldsymbol{Z}})/\mathrm{Tr}(\boldsymbol{D}_0\bar{\boldsymbol{Z}})$. On the other hand, it is reasonable to assume that $\boldsymbol{x} \neq \boldsymbol{s}_0$ such that $\|\boldsymbol{x} - \boldsymbol{s}_0\| > 0$ holds. Under this assumption, $\mathrm{Tr}(\boldsymbol{D}_0\boldsymbol{Z}) > 0$ holds. For any feasible $\boldsymbol{Z}$ of Problem (16), we can define a point $\bar{\boldsymbol{U}} = \boldsymbol{Z}/\mathrm{Tr}(\boldsymbol{D}_0\boldsymbol{Z})$. It is also easy to show that $\bar{\boldsymbol{U}}$ is feasible for Problem (17) and has the same objective value $\mathrm{Tr}(\boldsymbol{F}\bar{\boldsymbol{U}}) = \mathrm{Tr}(\boldsymbol{F}\boldsymbol{Z})/\mathrm{Tr}(\boldsymbol{D}_0\boldsymbol{Z})$. Thus, we conclude that Problems (16) and (17) are equivalent and the optimal solution of (16) can be obtained through (18). ■

The proposition indicates that Problem (16) can be solved by solving only one mixed SD/SOCP, thus significantly reducing the computational complexity. Moreover, it is worth noting that the proposed FP method only takes the target position as variable. This is different from the LLS and SDR methods in [24], which take both the target position and the clock skew as variables.

It is seen from the derivations that a known σ_δ^2 is required in the implementation of the proposed method. However, according to our assumption, σ_δ^2 is not known and only the upper bound δ_{max} is known. To obtain an approximate value of σ_δ^2 from δ_{max}, we suppose that δ follows a uniform distribution $\mathcal{U}(-\delta_{max}, \delta_{max})$ based on the known information that $\delta \in (-\delta_{max}, \delta_{max})$. By this assumption, we obtain an approximation to σ_δ^2, denoted by $\hat{\sigma}_\delta^2$, which is equal to $\hat{\sigma}_\delta^2 = \delta_{max}^2/3$. Replacing σ_δ^2 in $\boldsymbol{R}$ by $\hat{\sigma}_\delta^2$, we can obtain an approximation to $\boldsymbol{R}$, $\hat{\boldsymbol{R}}$, and $\hat{\boldsymbol{R}}$ is used in the whole implementation of the proposed method.

Remark 1: The mismatch between $\boldsymbol{R}$ and $\hat{\boldsymbol{R}}$ may degrade the performance of the WLS method (Eq. (10)). However, we see from the simulations that the proposed method is not sensitive to the inaccurate weighting matrix. This observation complies with the results in [7], [9], and [10].

Remark 2: Remark 1 shows that the way of using the known information of the upper bound on δ (i.e., δ_{max}) used in this paper is different from that in [24], in which this information is included as constraints in the optimization problem.

After solving the SD/SOCP (17), we can obtain the target position estimate $\boldsymbol{x}^* = \boldsymbol{Z}^*_{1:\ell,N+\ell+1}$. By using $\boldsymbol{x}^*$ and according to (4), we can estimate the clock skew w by solving the following problem:

$$
\begin{aligned}
\min_{\alpha} \ & (\boldsymbol{a} - \boldsymbol{d}\alpha)^T \boldsymbol{Q}^{-1} (\boldsymbol{a} - \boldsymbol{d}\alpha) \\
\text{s.t. } & \frac{1}{1+\delta_{max}} \leq \alpha \leq \frac{1}{1-\delta_{max}}, \qquad (19)
\end{aligned}
$$

where $\boldsymbol{a} = (\boldsymbol{r}^* - \boldsymbol{1}_N r_0^*) \otimes \boldsymbol{1}_K$ with $\boldsymbol{r}^* = [\|\boldsymbol{x}^* - \boldsymbol{s}_1\|, \ldots, \|\boldsymbol{x}^* - \boldsymbol{s}_N\|]^T$ and $r_0^* = \|\boldsymbol{x}^* - \boldsymbol{s}_0\|$. The estimate of w can be denoted by $w^* = 1/\alpha^*$ with α^* being the solution of (19).

IV. ANALYSIS

A. CRLB ANALYSIS

In this subsection, we derive a performance bound for the proposed method. Note that we cannot directly derive the CRLB based on the original measurement model (4) since we do not jointly estimate the target position and the clock skew. Hence, we need to transform the measurement model and derive a matched CRLB for the proposed method. To this end, we start transforming (4) as follows:

$$
\begin{aligned}
d_i^k &= w\left(\|\boldsymbol{x}^o - \boldsymbol{s}_i\| - \|\boldsymbol{x}^o - \boldsymbol{s}_0\| + n_i^k\right) \\
&= \|\boldsymbol{x}^o - \boldsymbol{s}_i\| - \|\boldsymbol{x}^o - \boldsymbol{s}_0\| \\
&\quad + \delta(\|\boldsymbol{x}^o - \boldsymbol{s}_i\| - \|\boldsymbol{x}^o - \boldsymbol{s}_0\|) + wn_i^k \\
&\approx \|\boldsymbol{x}^o - \boldsymbol{s}_i\| - \|\boldsymbol{x}^o - \boldsymbol{s}_0\| \\
&\quad + \delta(\|\boldsymbol{x}^o - \boldsymbol{s}_i\| - \|\boldsymbol{x}^o - \boldsymbol{s}_0\|) + n_i^k \\
&= \|\boldsymbol{x}^o - \boldsymbol{s}_i\| - \|\boldsymbol{x}^o - \boldsymbol{s}_0\| + \bar{e}_i^k, \qquad (20)
\end{aligned}
$$

where $\bar{e}_i^k = \delta(\|\boldsymbol{x}^o - \boldsymbol{s}_i\| - \|\boldsymbol{x}^o - \boldsymbol{s}_0\|) + n_i^k = \delta(r_i^o - r_0^o) + n_i^k$.

Note that (7) is an approximation to (20). Hence, we can derive the CRLB based on (20). In the following, we take $\bar{e}_i^k$ as the measurement noise. Moreover, to facilitate the derivation of CRLB, we assume that δ follows the Gaussian distribution with mean zero and variance σ_δ^2, and then $\bar{e}_i^k$ also follows a Gaussian distribution. Stacking $\bar{e}_i^k$ for $i = 1, \ldots, N$ and $k = 1, \ldots, K$ into vector $\bar{\boldsymbol{e}}$, we have $\bar{\boldsymbol{e}} = \boldsymbol{n} + \delta \boldsymbol{d}^o$, where $\boldsymbol{d}^o = (\boldsymbol{r}^o - r_0^o \mathbf{1}_N) \otimes \mathbf{1}_K$ with $\boldsymbol{r}^o = [r_1^o, \ldots, r_N^o]^T$. Obviously, $\bar{\boldsymbol{e}}$ follows the Gaussian distribution with mean zero and covariance $\bar{\boldsymbol{R}}$, where $\bar{\boldsymbol{R}} = \boldsymbol{Q} + \sigma_\delta^2 \boldsymbol{d}^o \boldsymbol{d}^{oT}$.

Now, it is easy to show that the expression of the CRLB is the same as that for TDOA-based localization in [7], i.e.,

$$\text{CRLB} = (\boldsymbol{C}^T \bar{\boldsymbol{R}}^{-1} \boldsymbol{C})^{-1}, \tag{21}$$

where

$$\boldsymbol{C} = \begin{bmatrix} \frac{(\boldsymbol{x}^o - \boldsymbol{s}_i)^T}{\|\boldsymbol{x}^o - \boldsymbol{s}_i\|} - \frac{(\boldsymbol{x}^o - \boldsymbol{s}_0)^T}{\|\boldsymbol{x}^o - \boldsymbol{s}_0\|} \\ \vdots \\ \frac{(\boldsymbol{x}^o - \boldsymbol{s}_i)^T}{\|\boldsymbol{x}^o - \boldsymbol{s}_i\|} - \frac{(\boldsymbol{x}^o - \boldsymbol{s}_0)^T}{\|\boldsymbol{x}^o - \boldsymbol{s}_0\|} \\ \vdots \\ \frac{(\boldsymbol{x}^o - \boldsymbol{s}_i)^T}{\|\boldsymbol{x}^o - \boldsymbol{s}_i\|} - \frac{(\boldsymbol{x}^o - \boldsymbol{s}_0)^T}{\|\boldsymbol{x}^o - \boldsymbol{s}_0\|} \\ \vdots \\ \frac{(\boldsymbol{x}^o - \boldsymbol{s}_i)^T}{\|\boldsymbol{x}^o - \boldsymbol{s}_i\|} - \frac{(\boldsymbol{x}^o - \boldsymbol{s}_0)^T}{\|\boldsymbol{x}^o - \boldsymbol{s}_0\|} \end{bmatrix}. \tag{22}$$

Remark 3: The exact value of σ_δ^2 is used in computing the CRLB (21). From Remark 1, we know that the exact value of σ_δ^2 is actually *not known* in implementing the FP method. Hence, the CRLB (21) is an overoptimistic lower bound for the MSE of the proposed method. This, in turn, implies that the FP method is *not* sensitive to the inaccurate σ_δ^2 if it could achieve the CRLB accuracy.

Remark 4: Comparing to the CRLB for joint estimation of the target position and the clock skew [24], the CRLB (21) is lower since the joint estimation methods in [24] estimate one more parameter, i.e., the clock skew.

B. MEAN SQUARE ERROR ANALYSIS

In this subsection, we derive the MSE of the original WLS method (Problem (10)) and show that the MSE can approach the CRLB at sufficiently small noise level.

Denote the optimal solution of Problem (10) as $\boldsymbol{x}^*$. According to the Karush-Kuhn-Tucker (KKT) optimality condition, we have

$$\boldsymbol{g}(\boldsymbol{x}^*) = \mathbf{0}_{\ell \times 1}, \tag{23}$$

where $\boldsymbol{g}(\boldsymbol{x}^*)$ is the gradient vector of $f(\boldsymbol{x})$ (defined in (10)) at $\boldsymbol{x}^*$.

Using the first-order Taylor-series expansion, we can approximate $\boldsymbol{g}(\boldsymbol{x}^*)$ as

$$\boldsymbol{g}(\boldsymbol{x}^*) \approx \boldsymbol{g}(\boldsymbol{x}^o) + \boldsymbol{H}(\boldsymbol{x}^o)(\boldsymbol{x}^* - \boldsymbol{x}^o) \approx \mathbf{0}, \tag{24}$$

where $\boldsymbol{g}(\boldsymbol{x}^o)$ and $\boldsymbol{H}(\boldsymbol{x}^o)$ are the gradient vector and the Hessian matrix at $\boldsymbol{x}^o$, respectively.

According to (24), we have

$$\boldsymbol{x}^* - \boldsymbol{x}^o \approx -\boldsymbol{H}(\boldsymbol{x}^o)^{-1} \boldsymbol{g}(\boldsymbol{x}^o). \tag{25}$$

The MSE of the estimate $\boldsymbol{x}^*$ is

$$\begin{aligned} \text{MSE} &= \mathbb{E}_{\boldsymbol{n}} \left[(\boldsymbol{x}^* - \boldsymbol{x}^o)(\boldsymbol{x}^* - \boldsymbol{x}^o)^T \right] \\ &\approx \mathbb{E}_{\boldsymbol{n}} \left\{ [\boldsymbol{H}(\boldsymbol{x}^o)^{-1} \boldsymbol{g}(\boldsymbol{x}^o)][\boldsymbol{H}(\boldsymbol{x}^o)^{-1} \boldsymbol{g}(\boldsymbol{x}^o)]^T \right\}. \end{aligned} \tag{26}$$

Using the definition of $f(\boldsymbol{x})$ in (10), we have

$$\begin{aligned} \boldsymbol{H}(\boldsymbol{x}^o) &= 2\boldsymbol{P}^T \boldsymbol{R}^{-1} \boldsymbol{P}, \\ \boldsymbol{g}(\boldsymbol{x}^o) &= -2\boldsymbol{P}^T \boldsymbol{R}^{-1} \boldsymbol{e}, \end{aligned} \tag{27}$$

where $\boldsymbol{P} = \partial \boldsymbol{\theta}(\boldsymbol{x}) / \partial \boldsymbol{x}^T |\boldsymbol{x} = \boldsymbol{x}^o$ and can be expressed as

$$\boldsymbol{P} = \begin{bmatrix} \frac{d_1^1 (\boldsymbol{x}^o - \boldsymbol{s}_i)^T}{\|\boldsymbol{x}^o - \boldsymbol{s}_0\| \|\boldsymbol{x}^o - \boldsymbol{s}_i\|} + \frac{(\boldsymbol{s}_i - \boldsymbol{s}_0)^T}{\|\boldsymbol{x}^o - \boldsymbol{s}_0\|} - \frac{e_1^1 (\boldsymbol{x}^o - \boldsymbol{s}_0)^T}{\|\boldsymbol{x}^o - \boldsymbol{s}_0\|^2} \\ \vdots \\ \frac{d_N^1 (\boldsymbol{x}^o - \boldsymbol{s}_i)^T}{\|\boldsymbol{x}^o - \boldsymbol{s}_0\| \|\boldsymbol{x}^o - \boldsymbol{s}_i\|} + \frac{(\boldsymbol{s}_i - \boldsymbol{s}_0)^T}{\|\boldsymbol{x}^o - \boldsymbol{s}_0\|} - \frac{e_N^1 (\boldsymbol{x}^o - \boldsymbol{s}_0)^T}{\|\boldsymbol{x}^o - \boldsymbol{s}_0\|^2} \\ \vdots \\ \frac{d_1^K (\boldsymbol{x}^o - \boldsymbol{s}_i)^T}{\|\boldsymbol{x}^o - \boldsymbol{s}_0\| \|\boldsymbol{x}^o - \boldsymbol{s}_i\|} + \frac{(\boldsymbol{s}_i - \boldsymbol{s}_0)^T}{\|\boldsymbol{x}^o - \boldsymbol{s}_0\|} - \frac{e_1^K (\boldsymbol{x}^o - \boldsymbol{s}_0)^T}{\|\boldsymbol{x}^o - \boldsymbol{s}_0\|^2} \\ \vdots \\ \frac{d_N^K (\boldsymbol{x}^o - \boldsymbol{s}_i)^T}{\|\boldsymbol{x}^o - \boldsymbol{s}_0\| \|\boldsymbol{x}^o - \boldsymbol{s}_i\|} + \frac{(\boldsymbol{s}_i - \boldsymbol{s}_0)^T}{\|\boldsymbol{x}^o - \boldsymbol{s}_0\|} - \frac{e_N^K (\boldsymbol{x}^o - \boldsymbol{s}_0)^T}{\|\boldsymbol{x}^o - \boldsymbol{s}_0\|^2} \end{bmatrix}. \tag{28}$$

Substituting d_i^k in (7) into (28), we can rewrite $\boldsymbol{P}$ as (29), as shown at the bottom of the next page.

At a sufficiently low noise level, we have $e_i^k \ll \|\boldsymbol{x}^o - \boldsymbol{s}_0\|$. Thus, $\boldsymbol{P}$ can be approximated by

$$\boldsymbol{P} \approx \begin{bmatrix} \frac{(\boldsymbol{x}^o - \boldsymbol{s}_0)^T}{\|\boldsymbol{x}^o - \boldsymbol{s}_0\|} - \frac{(\boldsymbol{x}^o - \boldsymbol{s}_i)^T}{\|\boldsymbol{x}^o - \boldsymbol{s}_i\|} \\ \vdots \\ \frac{(\boldsymbol{x}^o - \boldsymbol{s}_0)^T}{\|\boldsymbol{x}^o - \boldsymbol{s}_0\|} - \frac{(\boldsymbol{x}^o - \boldsymbol{s}_i)^T}{\|\boldsymbol{x}^o - \boldsymbol{s}_i\|} \\ \vdots \\ \frac{(\boldsymbol{x}^o - \boldsymbol{s}_0)^T}{\|\boldsymbol{x}^o - \boldsymbol{s}_0\|} - \frac{(\boldsymbol{x}^o - \boldsymbol{s}_i)^T}{\|\boldsymbol{x}^o - \boldsymbol{s}_i\|} \\ \vdots \\ \frac{(\boldsymbol{x}^o - \boldsymbol{s}_0)^T}{\|\boldsymbol{x}^o - \boldsymbol{s}_0\|} - \frac{(\boldsymbol{x}^o - \boldsymbol{s}_i)^T}{\|\boldsymbol{x}^o - \boldsymbol{s}_i\|} \end{bmatrix} = -\boldsymbol{C}. \tag{30}$$

Substituting (30) into (27) and then substituting (27) into (26), we have

$$\begin{aligned} \text{MSE}(\boldsymbol{x}^*) &\approx \mathbb{E}_{\boldsymbol{n}} \left\{ [\boldsymbol{H}(\boldsymbol{x}^o)^{-1} \boldsymbol{g}(\boldsymbol{x}^o)][\boldsymbol{H}(\boldsymbol{x}^o)^{-1} \boldsymbol{g}(\boldsymbol{x}^o)]^T \right\} \\ &= \mathbb{E}_{\boldsymbol{n}} \left[(\boldsymbol{P}^T \boldsymbol{R}^{-1} \boldsymbol{P})^{-1} \right]. \end{aligned} \tag{31}$$

It is easy to show that

$$\begin{aligned} \boldsymbol{R} &= \boldsymbol{Q} + \sigma_\delta^2 \boldsymbol{d}\boldsymbol{d}^T = \boldsymbol{Q} + \sigma_\delta^2 (\boldsymbol{d}^o + \boldsymbol{n})(\boldsymbol{d}^o + \boldsymbol{n})^T \\ &= \boldsymbol{Q} + \sigma_\delta^2 \boldsymbol{d}^o \boldsymbol{d}^{oT} + 2\sigma_\delta^2 \boldsymbol{d}^{oT} \boldsymbol{n} + \sigma_\delta^2 \boldsymbol{n}\boldsymbol{n}^T \\ &\approx \bar{\boldsymbol{R}} + 2\sigma_\delta^2 \boldsymbol{d}^{oT} \boldsymbol{n}, \end{aligned} \tag{32}$$

where the approximation is obtained by neglecting the second-noise term.

Substituting (32) into (31) yields

$$
\begin{aligned}
&\text{MSE}\\
&\approx \mathbb{E}_{\boldsymbol{n}}\left[(\boldsymbol{P}^T\boldsymbol{R}^{-1}\boldsymbol{P})^{-1}\right]\\
&= \mathbb{E}_{\boldsymbol{n}}\left\{\left[\boldsymbol{P}^T(\bar{\boldsymbol{R}}+2\sigma_\delta^2\boldsymbol{d}^{oT}\boldsymbol{n})^{-1}\boldsymbol{P}\right]^{-1}\right\}\\
&\approx \mathbb{E}_{\boldsymbol{n}}\left\{\left[\boldsymbol{P}^T(\bar{\boldsymbol{R}}^{-1}-2\sigma_\delta^2\bar{\boldsymbol{R}}^{-1}\boldsymbol{d}^{oT}\boldsymbol{n}\bar{\boldsymbol{R}}^{-1})\boldsymbol{P}\right]^{-1}\right\}\\
&\approx (\boldsymbol{P}^T\bar{\boldsymbol{R}}^{-1}\boldsymbol{P})^{-1}+2\sigma_\delta^2\\
&\quad\times\mathbb{E}_{\boldsymbol{n}}\left[(\boldsymbol{P}^T\bar{\boldsymbol{R}}^{-1}\boldsymbol{P})^{-1}\boldsymbol{P}^T\bar{\boldsymbol{R}}^{-1}\boldsymbol{d}^{oT}\boldsymbol{n}\bar{\boldsymbol{R}}^{-1}\boldsymbol{P}(\boldsymbol{P}^T\bar{\boldsymbol{R}}^{-1}\boldsymbol{P})^{-1}\right]\\
&= (\boldsymbol{P}^T\bar{\boldsymbol{R}}^{-1}\boldsymbol{P})^{-1}\\
&\approx (\boldsymbol{C}^T\bar{\boldsymbol{R}}^{-1}\boldsymbol{C})^{-1}\\
&= \text{CRLB}, \qquad (33)
\end{aligned}
$$

where the second and the third approximations follow from the approximation $(\boldsymbol{V}+\delta^2\boldsymbol{M})^{-1}\approx\boldsymbol{V}^{-1}-\delta^2\boldsymbol{V}^{-1}\boldsymbol{M}\boldsymbol{V}^{-1}$ for small δ^2.

C. COMPLEXITY ANALYSIS

The SD/SOCP (17) can be solved in polynomial time by an interior-point method [27, Lecture 6]. The worst-case computational complexity of solving an SD/SOCP is on the order of [25]

$$
\sqrt{\mu}\cdot\left(m\sum_{i=1}^{N_{\text{soc}}}(n_i^{\text{soc}})^2+m^2\sum_{i=1}^{N_{\text{sd}}}\left(n_i^{\text{sd}}\right)^2+m\sum_{i=1}^{N_{\text{sd}}}\left(n_i^{\text{sd}}\right)^3+m^3\right)\cdot\ln(1/\epsilon),
$$

where m is the number of equality constraints, N_{soc} (resp. N_{sd}) is the number of second-order cone (resp. semidefinite cone) constraints, n_i^{soc} (resp. n_i^{sd}) is the dimension of the ith second-order cone (resp. semidefinite cone),

$$
\mu=\sum_{i=1}^{N_{\text{sd}}}n_i^{\text{sd}}+2N_{\text{soc}}
$$

determines the order of iterations, and $\epsilon>0$ is the solution precision.

In (17), there are $4N+2$ equality constraints, 1 semidefinite cone of size $N+\ell+1$ (corresponding to (17d)), and N second-order cone constraints of size $\ell+1$ (corresponding to (17e)). Hence, the worst-case complexity of the proposed method is on the order of

$$
O\Big\{N^{0.5}\big[(4N+2)^2\left((N+\ell)^2+(4N+2)\right)+(4N+2)(N+\ell)^3\big]\Big\}\cdot\ln(1/\epsilon). \qquad (34)
$$

TABLE 1. Positions of the anchor nodes (unit: km).

Index	0	1	2	3	4	5	6	7	8
Anchor Positions	0 0	1 0	0 1	1 1	0 0.5	1 0.5	0.5 0	0.5 1	0.5 0.5

V. SIMULATION RESULTS

In this section, the performance of the proposed FP method (denoted by "FP") is validated through simulations. For comparison, the performance of the SDR method for solving the TOA based localization problem (denoted by "SDR-TOA") [23], the LLS and the SDR methods (denoted by "LLS" and "SDR", respectively) [24], and the robust SDR method [25] (denoted by "SDR-Robust") is included. The CRLB for joint estimation of the target position and the clock skew [24] (denoted by "CRLB-Joint"), the performance of the original WLS method (Problem (10)), and the CRLB (21) are also included as performance benchmarks. The positions of the anchors are listed in Table 1, and the position of the target is randomly and uniformly chosen from a square region of size $[0, 1.5]\times[0, 1.5]$ km^2. Note that the target may lie outside of the convex hull of the anchor positions. Taking $\boldsymbol{s}_0$ as the reference anchor, we generate the range measurements using the measurement model (4). In (4), w is randomly chosen according to the Gaussian distribution $\mathcal{N}(0, 0.003)$. The SD/SOCP (17) and the SDP in [24] are solved using MATLAB toolbox CVX [28], and the solver is SDPT3 [29]. The localization performance is evaluated in

$$
\boldsymbol{P}=\begin{bmatrix}
\frac{(\boldsymbol{x}^o-\boldsymbol{s}_0)^T}{\|\boldsymbol{x}^o-\boldsymbol{s}_0\|}-\frac{(\boldsymbol{x}^o-\boldsymbol{s}_i)^T}{\|\boldsymbol{x}^o-\boldsymbol{s}_i\|}+\frac{e_1^1(\boldsymbol{x}^o-\boldsymbol{s}_i)^T}{\|\boldsymbol{x}^o-\boldsymbol{s}_0\|\|\boldsymbol{x}^o-\boldsymbol{s}_i\|}-\frac{e_1^1(\boldsymbol{x}^o-\boldsymbol{s}_0)^T}{\|\boldsymbol{x}^o-\boldsymbol{s}_0\|^2}\\
\vdots\\
\frac{(\boldsymbol{x}^o-\boldsymbol{s}_0)^T}{\|\boldsymbol{x}^o-\boldsymbol{s}_0\|}-\frac{(\boldsymbol{x}^o-\boldsymbol{s}_i)^T}{\|\boldsymbol{x}^o-\boldsymbol{s}_i\|}+\frac{e_N^1(\boldsymbol{x}^o-\boldsymbol{s}_i)^T}{\|\boldsymbol{x}^o-\boldsymbol{s}_0\|\|\boldsymbol{x}^o-\boldsymbol{s}_i\|}-\frac{e_N^1(\boldsymbol{x}^o-\boldsymbol{s}_0)^T}{\|\boldsymbol{x}^o-\boldsymbol{s}_0\|^2}\\
\vdots\\
\frac{(\boldsymbol{x}^o-\boldsymbol{s}_0)^T}{\|\boldsymbol{x}^o-\boldsymbol{s}_0\|}-\frac{(\boldsymbol{x}^o-\boldsymbol{s}_i)^T}{\|\boldsymbol{x}^o-\boldsymbol{s}_i\|}+\frac{e_1^K(\boldsymbol{x}^o-\boldsymbol{s}_i)^T}{\|\boldsymbol{x}^o-\boldsymbol{s}_0\|\|\boldsymbol{x}^o-\boldsymbol{s}_i\|}-\frac{e_1^K(\boldsymbol{x}^o-\boldsymbol{s}_0)^T}{\|\boldsymbol{x}^o-\boldsymbol{s}_0\|^2}\\
\vdots\\
\frac{(\boldsymbol{x}^o-\boldsymbol{s}_0)^T}{\|\boldsymbol{x}^o-\boldsymbol{s}_0\|}-\frac{(\boldsymbol{x}^o-\boldsymbol{s}_i)^T}{\|\boldsymbol{x}^o-\boldsymbol{s}_i\|}+\frac{e_N^K(\boldsymbol{x}^o-\boldsymbol{s}_i)^T}{\|\boldsymbol{x}^o-\boldsymbol{s}_0\|\|\boldsymbol{x}^o-\boldsymbol{s}_i\|}-\frac{e_N^K(\boldsymbol{x}^o-\boldsymbol{s}_0)^T}{\|\boldsymbol{x}^o-\boldsymbol{s}_0\|^2}
\end{bmatrix}. \qquad (29)
$$

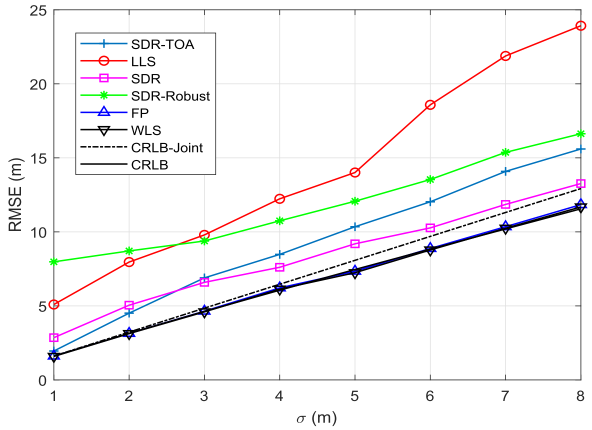

FIGURE 1. RMSE of the target position estimates versus the standard deviation of noise using different methods.

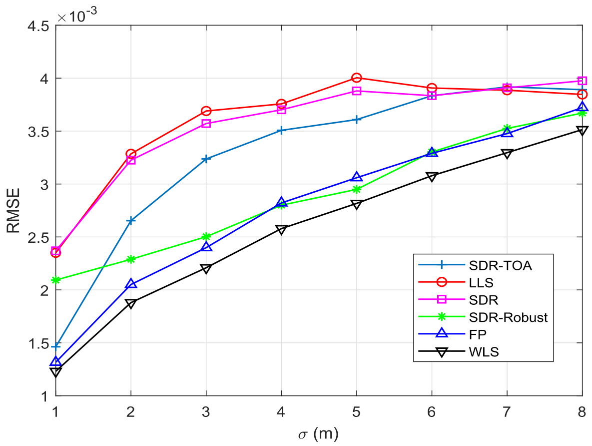

FIGURE 2. RMSE of the clock skew estimates versus the standard deviation of noise using different methods.

terms of root mean square error (RMSE), which is defined as

$$\text{RMSE} = \sqrt{\frac{1}{M}\sum_{i=1}^{M}\|\hat{\boldsymbol{x}}_i - \boldsymbol{x}_i\|^2}.$$

Here, M is the number of Monte Carlo (MC) runs and $\hat{\boldsymbol{x}}_i$ is the estimate of the true source location $\boldsymbol{x}_i$ in the ith run. In this paper, we use $M = 3000$ MC runs to evaluate the RMSE. Note that w follows a Gaussian distribution in the simulations, and its variance is not known in implementing the proposed method. In the simulations, we set $\delta_{max} = 2.5\sigma_\delta$, which yields an approximate $\hat{\sigma}_\delta^2$ equaling to $\delta_{max}^2/3 = 25\sigma_\delta^2/12$. Obviously, the approximate $\hat{\sigma}_\delta^2$ is not equal to σ_δ^2.

1) SCENARIO 1

In this scenario, we use eight anchors (Indices 0-7 in Table 1) to localize the target. We set $K = 4$ and vary the standard deviation (STD) of noise, σ, from 1 m to 8 m. Figs. 1 and 2 respectively show the RMSEs of the target position estimates and the clock skew estimates using different methods versus σ. From Fig. 1, we see that CRLB-Joint is lower than CRLB because joint estimation methods estimate one more parameter. The proposed method performs better than the other methods. Moreover, it performs comparably with the WLS method (Eq. (10)) and can approach the CRLB even though σ_δ^2 is not accurate, indicating that the proposed method is not sensitive to inaccurate σ_δ^2. It is worth noting that LLS and SDR require an additional step to further improve their performance. However, they still cannot achieve the CRLB accuracy (i.e., CRLB-Joint). In contrast, the proposed method does not need any postprocessing procedure. We observe from the simulations that FP is generally tighter than SDR. This can be attributed to the following two facts: (1) Minimizing the fraction in the objective function of the problem (16) is helpful to keep the relaxed problem tight. When minimizing the fraction, the denominator attempts to increase while the numerator attempts to decrease, thus helping keep $\boldsymbol{Z} \succeq 0$ tight; (2) The constraint $\|\boldsymbol{Z}_{1:k,N+k+1} - \boldsymbol{s}_i\| \leq Z_{i+k,N+k+1}$ also tightens the relaxed problem. From Fig. 2, we see that the proposed method also performs better than the other methods in estimating the clock skew.

TABLE 2. Number of MC runs with rank(z^*) = 1 for scenario 1 (3000 runs in total).

STD σ	1	2	3	4	5	6	7	8
Scenario 1	2983	2989	2995	2997	2994	2992	2990	2992

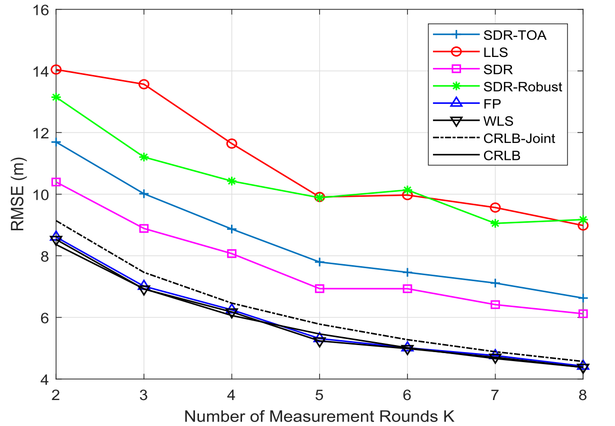

FIGURE 3. RMSE of the target position estimates versus the measurement rounds using different methods.

2) SCENARIO 2

Next, we examine the performance of the proposed method as the number of measurement rounds increases. We fix $\sigma = 4$ and $N = 7$, and increase the number of measurement rounds from $K = 2$ to $K = 8$. The simulation results are shown in Figs. 3 and 4, from which we see that the performance of all the methods improves as K increases. Moreover, FP provides almost 2 m reduction in target position estimation as compared with SDR, and also performs comparably or better as compared with the other methods in clock skew estimation.

3) SCENARIO 3

Finally, we consider the scenario when the number of anchors varies. We fix the values of σ and K as $\sigma = 4$ and $K = 4$, respectively, and vary the number of anchors from 6 ($N = 5$)

TABLE 3. Number of MC runs with rank(z^*) = 1 for scenario 2 (3000 runs in total).

No. of Measurement Rounds K	2	3	4	5	6	7	8
Scenario 2	2988	2991	2993	2992	2992	2995	2992

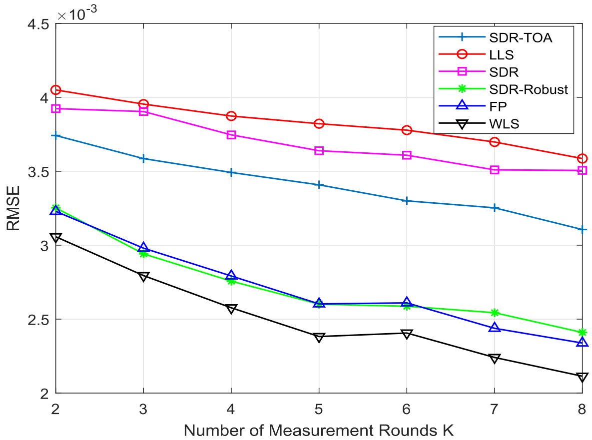

FIGURE 4. RMSE of the clock skew estimates versus the measurement rounds using different methods.

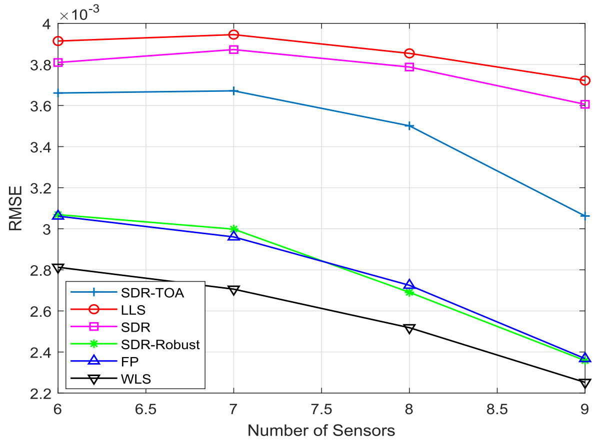

FIGURE 6. RMSE of the clock skew estimates versus the number of anchors using different methods.

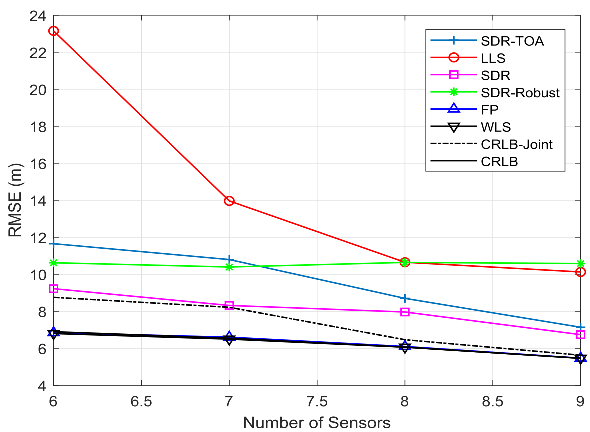

FIGURE 5. RMSE of the target position estimates versus the number of anchors using different methods.

TABLE 4. Number of MC runs with rank(z^*) = 1 for scenario 3 (3000 runs in total).

Number of Sensors	5	6	7	8
Scenario 3	2989	2994	2994	2991

to 9 ($N = 8$). The first $N + 1$ anchors in Table 1 are used. Figs. 5 and 6 show the simulation results in this scenario. From the figures, we see that the proposed robust method still performs better than the others, especially when the number of anchors is small. Specifically, when the number of the anchors is 5, FP provides a 3 m reduction in RMSE as compared to the other methods.

In Tables 2-4, we record the number of MC runs in which the SD/SOCP (17) yields a rank-1 solution $\boldsymbol{U}^{*1}$ and hence optimally solves the original WLS problem (10). From the tables, we see that the proportion of optimal solutions is very high. In all tested scenarios, SD/SOCP can yield the optimal solution to Problem (10) in more than 99.43% of the runs. This indicates that the relaxed SD/SOCP problem is almost always tight.

[1]We regard $\boldsymbol{U}^*$ to have rank 1 if the ratio between its second-largest and largest eigenvalue is less than 10^{-5}.

VI. CONCLUSION

In this paper, we have presented the FP method for target device localization. As compared with the traditional TDOA-based localization problem, the clock skew of the target still exists although the clock offset is eliminated. Unlike the existing SDR and LLS methods in [24], which jointly estimate the clock skew and the target position, we take the clock skew as a part of measurement noise and estimate the target position only. We then propose the novel FP method to estimate the target position. Different from the SDR and LLS methods in [24] that need a refined step to further improve their performance, the proposed method does not need any post processing procedure. Simulation results show that the proposed method achieves superior performance over the existing methods.

REFERENCES

[1] N. Patwari, J. N. Ash, S. Kyperountas, A. O. Hero, R. L. Moses, and N. S. Correal, "Locating the nodes: Cooperative localization in wireless sensor networks," *IEEE Signal Process. Mag.*, vol. 22, no. 4, pp. 54–69, Jul. 2005.

[2] N. Ansari, C. Zhang, R. Rojas-Cessa, P. Sakarindr, E. S. H. Hou, and S. De, "Networking for critical conditions," *IEEE Wireless Commun.*, vol. 15, no. 2, pp. 73–81, Apr. 2008.

[3] K. W. Cheung, W.-K. Ma, and H. C. So, "Accurate approximation algorithm for TOA-based maximum likelihood mobile location using semidefinite programming," in *Proc. IEEE Int. Conf. Acoustic, Speech, Signal Process.*, May 2004, p. 145.

[4] Y.-T. Chan, H. Yau Chin Hang, and P.-C. Ching, "Exact and approximate maximum likelihood localization algorithms," *IEEE Trans. Veh. Technol.*, vol. 55, no. 1, pp. 10–16, Jan. 2006.

[5] A. Beck, P. Stoica, and J. Li, "Exact and approximate solutions of source localization problems," *IEEE Trans. Signal Process.*, vol. 56, no. 5, pp. 1770–1778, May 2008.
[6] G. Wang, H. Chen, Y. Li, and N. Ansari, "NLOS error mitigation for TOA-based localization via convex relaxation," *IEEE Trans. Wireless Commun.*, vol. 13, no. 8, pp. 4119–4131, Aug. 2014.
[7] Y. T. Chan and K. C. Ho, "A simple and efficient estimator for hyperbolic location," *IEEE Trans. Signal Process.*, vol. 42, no. 8, pp. 1905–1915, Aug. 1994.
[8] K. Yang, G. Wang, and Z.-Q. Luo, "Efficient convex relaxation methods for robust target localization by a sensor network using time difference of arrivals," *IEEE Trans. Signal Process.*, vol. 57, no. 7, pp. 2775–2784, Jul. 2009.
[9] G. Wang *et al.*, "A semidefinite relaxation method for source localization using TDOA and FDOA measurements," *IEEE Trans. Veh. Technol.*, vol. 62, no. 2, pp. 853–862, Feb. 2013.
[10] G. Wang, S. Cai, Y. Li, and N. Ansari, "A bias-reduced nonlinear WLS Method for TDOA/FDOA based source localization," *IEEE Trans. Veh. Technol.*, vol. 65, no. 10, pp. 8603–8615, Oct. 2016.
[11] R. W. Ouyang, A. K.-S. Wong, and C.-T. Lea, "Received signal strength-based wireless localization via semidefinite programming: Noncooperative and cooperative schemes," *IEEE Trans. Veh. Technol.*, vol. 59, no. 3, pp. 1307–1318, Mar. 2010.
[12] G. Wang and K. Yang, "A new approach to sensor node localization using RSS measurements in wireless sensor networks," *IEEE Trans. Wireless Commun.*, vol. 10, no. 5, pp. 1389–1395, May 2011.
[13] G. Wang, H. Chen, Y. Li, and M. Jin, "On received-signal-strength based localization with unknown transmit power and path loss exponent," *IEEE Wireless Commun. Lett.*, vol. 1, no. 5, pp. 536–539, Oct. 2012.
[14] X. Guo and N. Ansari, "Localization by fusing a group of fingerprints via multiple antennas in indoor environment," *IEEE Trans. Veh. Technol.*, vol. 66, no. 11, pp. 9904–9915, Nov. 2017.
[15] X. Guo, L. Li, N. Ansari, and B. Liao, "Knowledge aided adaptive localization via global fusion profile," *IEEE Internet Things J.*, vol. 5, no. 2, pp. 1081–1089, Apr. 2018.
[16] Z. Chen, F. Xia, T. Huang, F. Bu, and H. Wang, "A localization method for the Internet of Things," *J. Supercomput.*, vol. 63, no. 3, pp. 657–674, 2013.
[17] Y.-C. Wu, Q. Chaudhari, and E. Serpedin, "Clock synchronization of wireless sensor networks," *IEEE Signal Process. Mag.*, vol. 28, no. 1, pp. 124–138, Jan. 2011.
[18] J. Zheng and Y.-C. Wu, "Joint time synchronization and localization of an unkown node in wireless sensor networks," *IEEE Trans. Signal Process.*, vol. 58, no. 3, pp. 1309–1320, Mar. 2010.
[19] A. Ahmad, E. Serpedin, H. Nounou, and M. Nounou, "Joint node localization and time-varying clock synchronization in wireless sensor networks," *IEEE Trans. Wireless Commun.*, vol. 12, no. 10, pp. 5322–5333, Oct. 2013.
[20] Y. Wang, X. Ma, and G. Leus, "Robust time-based localization for asynchronous network," *IEEE Trans. Signal Process.*, vol. 59, no. 9, pp. 4397–4410, Sep. 2011.
[21] M. R. Gholami, S. Gezici, and E. G. Storm, "Range based sensor node localization in the presence of unknown clock skews," in *Proc. IEEE Int. Conf. Acoust., Speech Signal Process. (ICASSP)*, 2013, pp. 4046–4050.
[22] S. Gao, S. Zhang, G. Wang, and Y. Li, "Robust second-order cone relaxation for TW-TOA-based localization with clock imperfection," *IEEE Signal Process. Lett.*, vol. 23, no. 8, pp. 1047–1051, Aug. 2016.
[23] R. M. Vaghefi and R. M. Buehrer, "Cooperative joint synchronization and localization in wireless sensor networks," *IEEE Trans. Signal Process.*, vol. 63, no. 14, pp. 3615–3627, Jul. 2015.
[24] M. R. Gholami, S. Gezici, and E. G. Strom, "TDOA based positioning in the presence of unknown clock skew," *IEEE Trans. Commun.*, vol. 61, no. 6, pp. 2522–2534, Jun. 2013.
[25] G. Wang, A. M.-C. So, and Y. Li, "Robust convex approximation methods for TDOA-based localization under NLOS conditions," *IEEE Trans. Signal Process.*, vol. 64, no. 13, pp. 3281–3296, Jul. 2016.
[26] S. Boyd and L. Vandenberghe, *Convex Optimization*. Cambridge, U.K.: Cambridge Univ. Press, 2004.
[27] A. Ben-Tal and A. Nemirovski, *Lectures on Modern Convex Optimization: Analysis, Algorithms, and Engineering Applications* (MPS-SIAM Series on Optimization). Philadelphia, PA, USA: SIAM, 2001.
[28] M. Grant and S. Boyd. *CVX: MATLAB Software for Disciplined Convex Programming, Version 2.1*. Accessed: Dec. 2017. [Online]. Available: http://cvxr.com/cvx
[29] K.-C. Toh, M. J. Todd, and R. H. Tutuncu, "On the implementation and usage of SDPT3—A MATLAB software package for semidefinite-quadratic-linear programming, version 4.0," in *Handbook on Semidefinite, Conic and Polynomial Optimization* (International Series in Operations Research & Management Science), vol. 166, M. F. Anjos and J. B. Lasserre, Eds. New York, NY, USA: Springer, 2012, pp. 715–754.

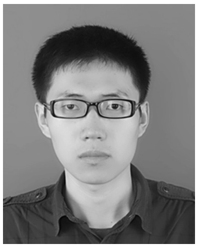

GANG WANG (M'13) received the B.Eng. degree from Shandong University, Jinan, China, and the Ph.D. degree from Xidian University, Xi'an, China, both in electrical engineering, in 2006 and 2011, respectively. He joined Ningbo University, Ningbo, China, in 2012, where he is currently an Associate Professor. His research interests are in the area of target localization and tracking in wireless networks.

NIRWAN ANSARI (S'78–M'83–SM'94–F'09) received the Ph.D. degree from Purdue University, West Lafayette, IN, USA, the M.S.E.E. degree from the University of Michigan, Ann Arbor, MI, USA, and the B.S.E.E. *(summa cum laude)* with a perfect GPA from NJIT, Newark, NJ, USA. He is currently a Distinguished Professor of electrical and computer engineering with the New Jersey Institute of Technology. He has also been a visiting (Chair) Professor at several universities. He has recently authored *Green Mobile Networks: A Networking Perspective* (IEEE-Wiley, 2017) under the supervision of T. Han, and co-authored two other books. He has also been granted 37 U.S. patents. He has also co-authored over 550 technical publications, over 250 published in widely cited journals/magazines. He has guest-edited a number of special issues covering various emerging topics in communications and networking. His current research focuses on green communications and networking, cloud computing, drone-assisted networking, and various aspects of broadband networks. Some of his recognitions include several Excellence in Teaching Awards, a few Best Paper Awards, the NCE Excellence in Research Award, the ComSoc TC-CSR Distinguished Technical Achievement Award, the ComSoc AHSN TC Technical Recognition Award, the IEEE TCGCC Distinguished Technical Achievement Recognition Award, the NJ Inventors Hall of Fame Inventor of the Year Award, the Thomas Alva Edison Patent Award, Purdue University Outstanding Electrical and Computer Engineer Award, and the designation as a COMSOC Distinguished Lecturer. He has chaired some ComSoc technical and steering committees, and has been serving in many committees such as the IEEE Fellow Committee. He was elected to serve in the IEEE Communications Society (ComSoc) Board of Governors as a member-at-large. He has served on the editorial/advisory board of over ten journals including as Senior Technical Editor of the *IEEE Communications Magazine*. He has been actively organizing numerous IEEE International Conferences, Symposia, and Workshops. He has frequently been delivering keynote addresses, distinguished lectures, tutorials, and invited talks.

YOUMING LI received the B.S. degree in computational mathematics from Lanzhou University, China, in 1985, the M.S. degree in computational mathematics from Xi'an Jiaotong University, Xi'an, China, in 1988, and the Ph.D. degree in electrical Engineering from Xidian University, Xi'an, China, in 1995. From 1988 to 1998, he was with the Department of Applied Mathematics, Xidian University, where he was an Associate Professor. From 1999 to 2004, he was with the DSO National Laboratories, School of Electrical and Electronics Engineering, Nanyang Technological University, Singapore, and the School of Engineering, Bar-Ilan University, Israel, respectively. Since 2005, he has been with Ningbo University, Ningbo, China, where he is currently a Professor. His research interests are in cognitive radio and wireless/wireline communications.